Research on Engineering Structures & Materials

journal homepage: http://www.jresm.org

Research Group

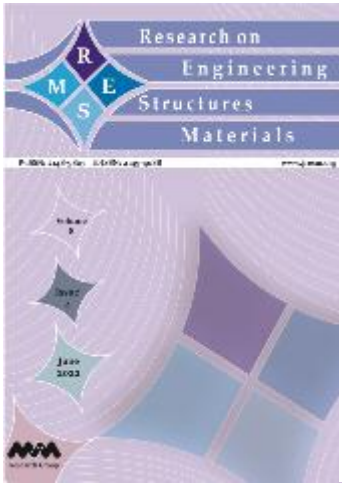

Analytical study on seismic strengthening of existing reinforced concrete buildings by implementation of energy absorbers

Mehmet Cemal Geneş, Pari Yaseen

Online Publication Date: 10 June 2023
URL: http://www.jresm.org/archive/resm2023.677ea0129.html
DOI: http://dx.doi.org/10.17515/resm2023.677ea0129

Journal Abbreviation: *Res. Eng. Struct. Mater.*

To cite this article
Genes MC, Yaseen P. Analytical study on seismic strengthening of existing reinforced concrete buildings by implementation of energy absorbers. *Res. Eng. Struct. Mater.*, 2023; 9(4): 1543-1571.

Research on Engineering Structures & Materials
journal homepage: http://www.jresm.org
Research Group

Research Article

Analytical study on seismic strengthening of existing reinforced concrete buildings by implementation of energy absorbers

Mehmet Cemal Geneş*[a], Pari Yaseen[b]

Civil Engineering Department, Eastern Mediterranean University, Famagusta, Cyprus via Mersin 10, Turkey

Article Info

Article history:

Received 29 Jan 2023
Accepted 03 Jun 2023

Keywords:

Nonlinear time history; analysis; Hysteretic; Absorbers; Energy; Dissipating devices; Seismic strengthening; Seismic risk

Abstract

Retrofitting of reinforced concrete (RC) buildings is generally made by jacketing of columns and/or implementing shear walls. However, this method increases the building mass and requires foundation strengthening which is not easy to apply. Recently, strengthening by absorbing the applied energy to the building during an earthquake by energy absorbers has become popular. In this study, an analytical study of an energy dissipation system for seismic strengthening of existing RC buildings is presented. The study was conducted to investigate the implementation of an energy absorber to the bracing system of an existing building located in Antakya/Türkiye. One of the considerable challenges is to establish the optimal design to retrofit buildings against the effect of predicted earthquakes with minimal disturbance to the structure and residents. The proposed system aims to provide high protection of the structure during severe earthquakes by controlling the maximum inter-story drifts. The used system performs as a bilinear hysteretic device. To investigate the performance of the proposed design and configuration, nonlinear time-history analyses were carried out on an 8-Story building. The main parameters which are Displacement, Inter Story Drift Ratio, Acceleration, and Input Energy are studied according to the different configurations. The obtained results showed that the seismic responses of the strengthened structures were significantly higher than the original structures. The maximum displacement and drift reduction values of the strengthened building were between 70% to 80%, the maximum acceleration reduction values were between 4% to 20%, and the input energy levels decreased between about 64% and 70%.

1. Introduction

When a severe earthquake occurs near residential areas, it can cause damage to reinforced concrete (RC) structures and result in life and property losses. Furthermore, structural and nonstructural damages are essentially due to lateral displacements and acceleration [1]. Therefore, structures are required to be strong enough to resist seismic effects.

There is a seismic activity zone in Türkiye that ranks second on the planet which is known as the Alpine-Himalayan Belt. The highest level of seismic activity in Türkiye was known to be up to 0.8g. But after the 6th February 2023 Kahramanmaraş earthquakes depending on soil conditions the seismic activity could be more than 1.3g.

The major plate in which Türkiye is known as the Anatolian plate as shown in Figure 1. It is bounded by two great strike-slip fault zones, the 550 km-long East Anatolian Fault and the 1500 km-long North Anatolian Fault [2]. The fault as a result of the collision, the Anatolian Plate was formed of the complicated zone between the Eurasian Plate and both the Arabian and African Plates [3].

*Corresponding author: cemal.genes@emu.edu.tr
[a] orcid.org/0000-0002-9052-7361; [b]orcid.org/0000-0001-7292-7049
DOI: http://dx.doi.org/10.17515/resm2023.677ea0129

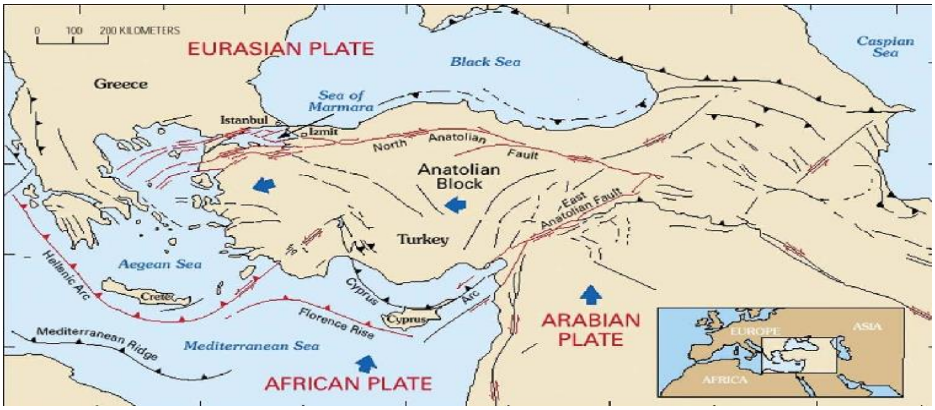

Fig. 1 Tectonic map of Türkiye [2]

Due to these fault ruptures, more than 800 earthquakes with various magnitudes have occurred in the last 120 years in Türkiye as given in Table 1 according to the obtained data from the Disaster and Emergency Management Presidency Earthquake Department (AFAD). However, after the recent earthquakes in Kahramanmaraş (M_w:7.7 and M_w:7.6) and Hatay (M_w:6.4), Table 1 should be modified with a new number of events which are shown in brackets.

Table 1. Past earthquakes in Türkiye between 1900 and 2020 [4]

Earthquake Magnitude	6 > M ≥ 5	7 > M ≥ 6	M > 7
No. of Events	702	81 (82)	17 (19)
Return Interval (years)	0.2	1.5	7

Moreover, due to the continued convergence between Eurasian Plate and both the Arabian and African Plates, there is generated energy that is stored and can be released at any moment in the form of considerable earthquakes magnitude. Therefore, at least one major earthquake of magnitude ≥ 7.0 can occur in the future [5, 6]. The major earthquake return period in Türkiye is around seven years according to AFAD which is a very short-term return interval for a major earthquake. In general, an earthquake magnitude between 7.0 and 7.9 is considered a considerable earthquake that can cause severe damage or collapse of buildings, injuries, as well as pose a risk to lives [7].

The existing buildings have much more crucial seismic resistance problems in comparison to the buildings that have been designed during recent 25 years according to seismic precautions. The buildings have been designed according to older codes, which primarily focus on resisting gravity loads only. The buildings which have been constructed in high seismic zones, if they are designed to resist earthquakes according to seismic codes, can resist the earthquake loads adequately [1, 8]. Moreover, the past forty years have witnessed a considerable increase in awareness about earthquake engineering that indeed modern structures don't meet the requirements of constantly evolving codes. Therefore, several deficiencies can be found in existing structures as well as inadequate lateral stiffness, irregular structural configuration, and inappropriate member detailing for ductility. However, the issue becomes more sophisticated when other aspects, beyond the reach of codes, are taken into consideration. Generally, it is usual for the owners of existing buildings to have structural modifications without any engineering consideration, resulting in further obstruction of the structures which might already have low seismic resistance. In addition, the construction quality may be poor because of deficient design

and execution. Thus, buildings that have seismic deficiencies may cause injuries and casualties besides economic loss [9]. Most of the existing buildings, which are older than 30 years in Türkiye, have been designed and constructed without or with weak methods of seismic resistance precautions. Therefore, the buildings are most likely to experience severe damage even when mild earthquake events occur. To resist earthquakes and prevent failure of the structures, strengthening both old buildings that have been designed according to old codes and new buildings designed according to recent codes but have insufficient seismic-resistant is critically needed.

A preliminary step in seismic strengthening is determining the essential structural characteristics of existing buildings as well as their earthquake resistance capacity. After that, rehabilitation performance objectives are set, and the seismic hazard level is determined, accordingly. However, it's not simple to work since complicated cooperation needs to be considered between technical, economic, and social factors, specified for each region. The social factor is considered by the decision on the performance level of the building seismic appraisal and retrofitting. According to engineering judgment, the most appropriate measures can be selected to improve the structure's behavior. In general, local evaluations are more suitable when some structure's components have inadequate capacity, while comprehensive measures are appropriate in case of major deformation, including irregularities and pounding. The Federal Emergency Management Agency (FEMA) using Seismic Techniques, Rehabilitation of Existing Structures can be used as guidance for Seismic Assessment and Retrofit [9].

The protection of buildings in seismically active zones is required to meet the following requirements:

a. The main system of the structure must have adequate resistance to be able to withstand medium-intensity earthquakes without being damaged, which can impact the structure at least once.

b. All the structure's elements should have ductility to decrease seismic input energy without collapse.

Modern structures can achieve these strengths and ductility benefits without anti-seismic devices if certain design and execution principles are adhered to. Conversely, buildings and structures built according to the old codes don't have high ductility, and even conventional strengthening techniques don't enhance ductility as they are primarily focused on resistance in the elastic range. Therefore, to achieve a sufficient response to seismic activity or to reduce the structure's vulnerability, the energy can be dissipated through the implementation of the structural control system.

To achieve seismic design, probabilistic analysis is essential because of the large uncertainties associated with forces and structural responses [10]. Moreover, it is not possible to predict the earthquake's occurrence, its magnitude, the features of the rupture surface, and the structure's dynamic response with absolute certainty. Therefore, to evaluate the impact of these uncertainties on the performance of structures and seismic design, probabilistic and statistical methods are required. The other essential seismic engineering concept is that materials must be designed and prepared to behave inelastically due to severe earthquake loading. The relationship between stress and strain is linear within Hooke's Law, but beyond this point, structural behavior becomes more complicated. Moreover, the Inelastic behavior of structures was largely investigated using analytical and experimental techniques established around the 1960s [11].

The earthquake-resistant design incorporates various types of seismic control systems to decrease the effects of seismic forces on the building's essential structural elements. In

general, structural control systems are classified into four general types based on the user device types: active, semi-active, hybrid, and passive [12].

Currently, seismic control devices are the most reliable and functional methods to reduce a structure's seismic response. Installing seismic control devices in a structure provides artificially increase structural damping, consumes the vibration energy under the earthquake, reduces the vibration response, and achieves the purpose of earthquake resistance of the structure. The effectiveness of these systems is highlighted through a detailed earthquake damage assessment, there can be a considerable reduction of seismic impacts on the main structure to be protected [13, 14]. One of the seismic controllers is energy dissipation devices, they are mechanical systems that are linked to the building frame to allow the structure to withstand earthquake shaking by absorbing a considerable amount of energy input resulting from seismic activity, without deforming and yielding [15]. Different types of energy dissipation systems are classified according to their ability to improve structural system dissipation energy.

The energy-dissipating devices in framed structures are generally inserted in braces of steel between two sequent stories of the structure as shown in Figure 2. The inter-story drifts accommodated by the building when a seismic event occurs stimulate the energy-dissipating devices before the essential members of the structure are involved in their inelastic behavior. Accordingly, the main objective of the current design strategy employed for energy-dissipating devices is to substantially reduce the demands for ductility on structural members made of RC as stated by Dolce et al. [16]. Thus, the system that supports gravity loads and the system that dissipates energy during an earthquake are discrete systems.

According to a study by Reinhorn et al. [17], it has been shown that the implementation of energy dissipation devices greatly improves the overall capacity of old seismic codes or RC frame structures designed to bear gravity loads. The energy-dissipating devices initially depend on the plastic hinges developed for columns that have low energy dispersal capacity and rapidly deteriorate in rigidity and strength. Accordingly, it's observed that structural vibrations have been significantly reduced [18].

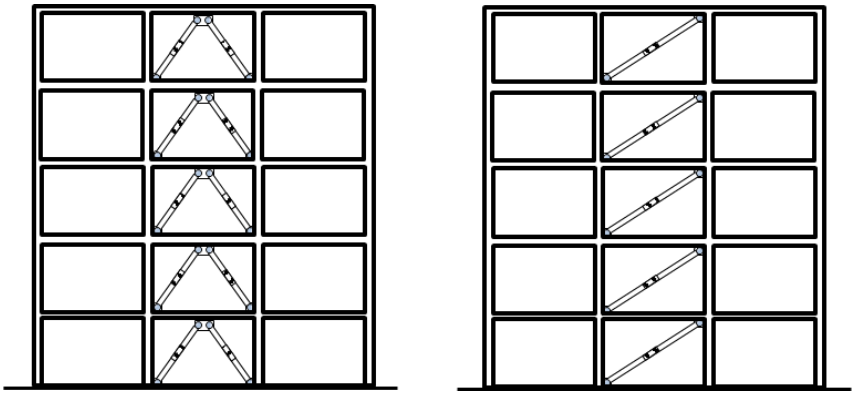

Fig. 2 Energy dissipation system in a structure [18]

There are several energy dissipation devices have been studied by scientist and some of them are applied in newly designed and strengthened buildings. These devices are Metallic Yielding Dampers [19, 20, 21], Energy Dissipative Bracing (EDB) [22, 13, 23, 24], Hysteretic Energy Dissipative Bracing (HEDB) [25, 26] , Dissipative Energy Device Based on The Plasticity of Metals [15], Seismic Design of RC Braced Frames with Metallic Fuses [27, 28],

Saw Type Seismic Energy Dissipaters [29, 30], Re-centering Energy Dissipative Braces [31] and Adaptive Hysteretic Dampers [32], Impulsive Semi-Active Mass Dampers [33], Damped Braces [34], bolt connected buckling-restrained braces [35] [36] and visco-elastic dampers [37].

A new metallic-yielding pistonic (MYP) damper is presented by Ghandil et al. [21] for seismic control of structures. A set of rectangular metallic yielding plates has been considered as an energy-dissipating part of this damper. According to its yielding mechanism and its special configuration, the story high-performance in seismic protection of structures at low-value story drifts is presented.

Thongchom et al. [38, 28] proposed a new metallic damper consisting of five plates: shear plate, flange plate, X-stiffeners, middle plate, and boundary plates. The middle plate and boundary plates do not contribute to resisting the applied load while the shear plate, flange plate, and X-stiffeners share the shear strength.

In order to demonstrate the effectiveness of the dampers Zhu et al. [39] performed an experimental and numerical study of an X-type energy dissipation device under impact loads. They tested 20 specimens by using a drop hammer impact test machine, then established a model with finite elements by using the software LS-DYNA.

Due to its stable hysteretic behavior and the ability to transfer the inter-story shear force or axial load of a brace into the moment of the steel plate many analytical, experimental, and optimization studies were carried out [40].

In the present research, a seismic control technique that is based on Hysteretic Dissipative Energy Bracing Based on the plasticity of metals is used. The brand and name of the energy damper are MAURER and SHARK (Short-stroke Hysteretic Damper jacK) [41], respectively. The energy dissipation system is incorporated into an existing reinforced concrete building located in Türkiye. This seismic system is developed to enhance the seismic performance of buildings by limiting inter-story drift while preventing the damage of the structure. Nonlinear Time-History Analysis is conducted to investigate the system performance to decrease the input energy, inter-story drift, top displacement, and top acceleration.

The main aim of this study is to introduce and recommend seismic control techniques for existing RC buildings to withstand minor earthquakes and avoid major damage and collapse during a severe earthquake. A strengthening procedure involves technical interventions in a building's structure that increase its structural stiffness, strength, or/and ductility to increase its seismic resistance. Furthermore, increase awareness about earthquake impact on existing buildings in highly seismic areas of Türkiye and assure knowledge in design and seismic rehabilitation. In addition, the strengthening existing structures assures to keep human life is safe, and that occupants or pedestrians will not be injured by a collapsed structure. Consequently, this study sought to define a design procedure for seismic retrofitting of existing RC-framed buildings using an energy dissipation device based on hysteretic damping.

The proposed study is carried out in two stages which include, collecting data and model analysis. Stage one is carried out to collect data about the selected building structure, seismic area, earthquake records, ambient vibration records [42] and the used energy absorber. The collected data was utilized in the second stage to develop and estimate an accurate calibrated three-dimensional model to perform analysis through ETABS software, in which the buildings configurations were modeled, the contribution of earthquakes and their impact on the structure of the building were elaborately investigated under Nonlinear Time History Analysis (NLTHA) considering and comparing the existing framed

building and the strengthened framed building by the implementation of SHARK energy dissipation device.

2. Research Methodology

A three-stage process is followed in this research methodology. The first stage consists of designing a building with different configurations and materials to calibrate the model and define the current performance of the building. The second stage consists of the implementation of the SHARK energy dissipation device in the braced frame of the designed building in different installation configurations. Finally, the third stage consists of evaluating the performance of the original and the strengthened building and comparing them based on the results obtained from nonlinear time-history analyses by applying 11 pairs of earthquakes to the buildings.

2.1. Introducing the Used Building Bracing System

SHARK is an inventive energy dissipation device that can provide absolute structural safety and reduce the risk of potential damage caused by earthquakes. The design, testing, and quality management of the bracing system comply according to [43]. The SHARK device shown in Figure 3 is made of steel. Its innovative design represents a simple but extremely efficient energy dissipation. When the structure is subjected to loads, the damper operates within its elastic system and acts as a rigid spring to provide structural support. When an earthquake occurs, the SHARK's specially shaped hysteretic lamellas experience plastic deformation to dissipate seismic energy. On the four faces of the hollow section of the dissipative core shown in Figure 3. For severe Ultimate Limit State (ULS) earthquakes, the damper provides stable and reliable performance. The damper can endure up to 3-4 MCE events without any failure due to the special shape of the lamellas. After an unavoidable failure of one lamella, the rest offer proportional resistance and damping functions. The configuration of SHARK is shown in Figure 4. Table 2 provides the size and performance data of SHARK. Furthermore, there is a second form known as SHARK-Adaptive which minimizes the accelerations at each level to ensure better protection of sensitive non-structural components. The SHARK-Adaptive damper features a unique “two-stage” hysteretic loop that allows for the adjustment of effective stiffness and damping based on the intensity of the earthquake [41].

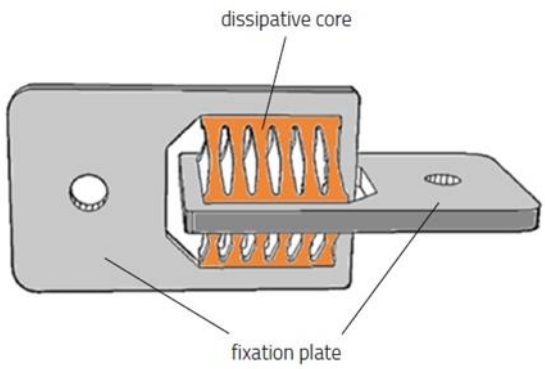

Fig. 3 SHARK damper dissipation core and fixation plate [41]

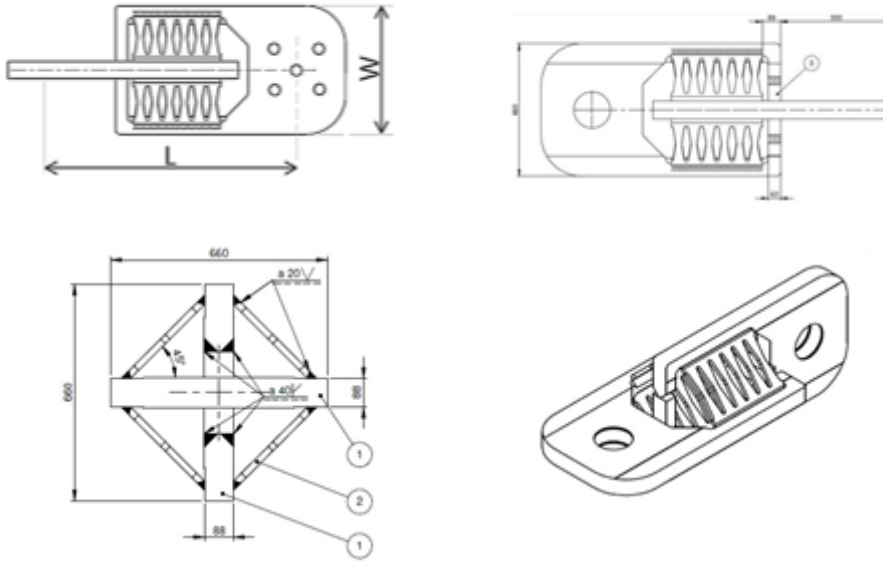

Fig. 4 MAURER SHARK (a) Configuration, (b) side view, (c) front view, (d) 3D view [41]

Table 2. Size and performance data of SHARK [41]

FMCE [kN] MASS	FYk [kN]	K_{el} [kN/mm]	K_{pl} [kN/mm]	dSLS [±mm]	dMCE [±mm]	d_{cd} [±mm]	L [mm]	W [mm]	d_y [mm]	F_{pl} (kN)
350	220	100	4	≤ 1	35	50	700	560	2.2	411.2
700	410	165	6	≤ 1	50	70	800	580	2.484	815.1
1000	615	245	9	≤ 1	50	70	900	600	2.510	1222.4
1400	820	325	12	≤ 1	50	70	1000	620	2.523	1629.7
1700	1020	410	15	≤ 1	50	70	1100	640	2.487	2032.7
2100	1230	490	18	≤ 1	50	70	1200	660	2.510	2444.8
2400	1430	570	21	≤ 1	50	70	1300	680	2.508	2847.3

The utilizing of the SHARK energy dissipation device has the following advantages: There is no need for regular maintenance and the use of only one material provides high reliability, The building structural systems have a similar service life, provide stable response of up to 3-4 MCE earthquake events without any failure [41], high level of safety due to the parallel configuration of hysteretic lamellas, uncomplicated bilinear model appropriate for analysis, having a compact size, a convenient visual inspection and replacement process if needed after a fire or other unforeseen event, exceptional fatigue strength in case of wind, as well as service loads, design following European Standard EN15129 or according to other standards upon request.

A typical installation layout is illustrated by two examples in Figure 5. In general, the connection to the construction can be screwed or welded, as appropriate for the project, it also can be connected directly to the original frame of the building by connections to the middle of the beam and ends of the columns [41]. However, as there is an additional shear force in the beam, particularly because of this diagonal force, the shear force should be transferred to the beam element by applying steel jacketing around the beam to show the

effectiveness of the connections to transfer the loads. For this study, installation layout A is applied to the buildings, and according to the first data provided in Table 3.

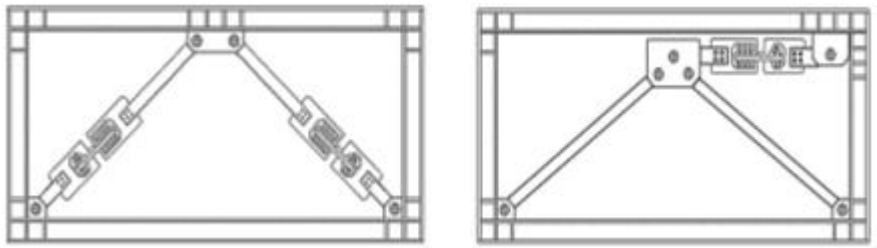

Fig. 5 Installation layout A and B [41]

The performance of the SHARK has been successfully tested as shown in Figure 6 and, showed a perfect hysteretic loop according to the European Standard EN 15129 at EUCENTRE Laboratory in Pavia (Italy) and Bundeswehr University of Munich. As part of nonlinear finite element analysis, SHARK has been designed and optimized [41, 32].

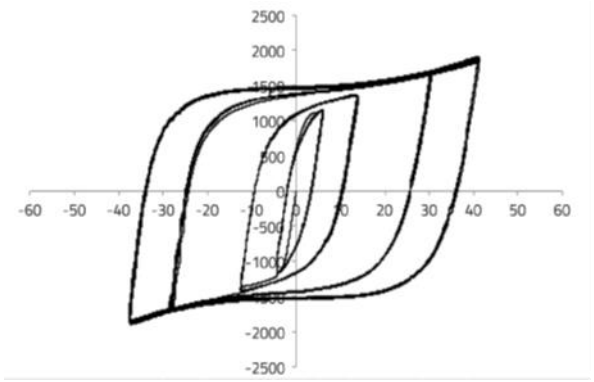

Fig. 6 Experimental bilinear hysteretic loop of Shark [41]

2.2 Modelling of Studied Building

The studied building was built in 1973 in Antakya/Hatay (Figure 7). In the frame of a project which is supported by TUBITAK with a project code TUBITAK (107M445), the building was studied by providing ambient vibration to calibrate its model and performing pushover analysis to define its performance level. During that project study, the project team found that this building has characteristic features that can represent approximately 71 of the reinforced concrete buildings in Antakya [42]. There are two apartments on each floor of the building. Therefore, it is not symmetrical concerning the X-axis.

The cross-section dimensions of the column elements used while modeling are given in Table 3. The building is an 8-story RC frame, with a height of 2.9 meters for each story. The total height of the structure above the basement is 23.2 meters. There is no earthquake-resisting shear walls or reinforced concrete core around the elevator in the building. There are 17 columns, and the sections and reinforcement ratios of these columns vary between stories. C16 concrete and St-I (S220) reinforcing steel properties were used in the modeling of the building. According to the region where the building is located (the

coordinate is Latitude: 36.210103° Longitude 36.159782°), the ground condition is very tight layers of sand, gravel, and hard clay or weathered, very cracked weak rocks [42].

Fig. 7 The studied apartment building

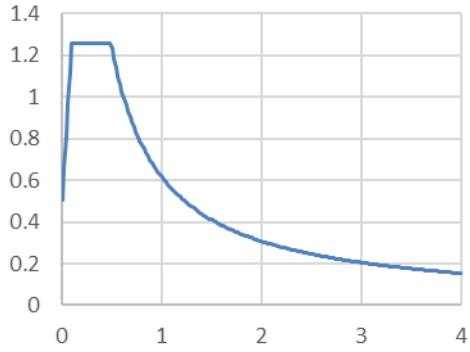

Fig. 8 The target response spectrum of soil class C

ETABS software has been used to create a three-dimensional model design and perform analysis. ETABS follows [44] to employ the performance-based design of the lateral load-bearing systems. According to TBEC-2018 [45], the soil class "C" is considered to define the spectrum curve of the site. Therefore, Figure 8 presents the target response spectrum curve corresponding to this region.

The ACI-318-11 [44] and ASCE 41-17 [46] design codes have been utilized in the design of the reinforced concrete building, and all details have been observed and considered according to these standards. Hinges were assigned according to [46]. Table 3 and Figure 9 illustrate the frame section property definitions of the members used in the modelling and analysis.

The dead and live loads based on the residential use of the building are used as 4.2 kN/m^2 and 2 kN/m^2, respectively. The design of the 8-story building is conducted according to the specified plan and sections without considering the infill walls. However, according to the original plan, there are balconies along the X-axis which prevent the possibility of energy absorber implementation. Therefore, the balconies on the edges of the X-axis are removed and the energy absorber is applied on the edges. Further, an analysis was conducted to define the structure's dynamic behavior parameters (vibration periods and mode shapes) and compare them with the real parameters obtained from the study of [42] to calibrate the analytical model of the building, and then to determine and evaluate the behavior of the strengthened structure with SHARK energy dissipator. The obtained vibration periods and frequencies after model calibration are presented in Table 4. The building model and the plan layout are presented in Figure 10.

The load combinations have been considered following [45] regulations to analyze the building.

As is clear from the 3D model and plan of the building (Figure 10), the building does not have a strong earthquake resistance system (i.e. Shear walls or RC core). The performance analysis results of the building are given in Table 5 and Figure 11. According to the results, the 4th floor of the building has a performance level of failure, as severely damaged columns are formed and all the shear forces on this floor are carried by the damaged columns.

According to the Turkish Building Earthquake Code [45] and Türkiye Earthquake Hazard Maps Interactive Web Application (AFAD), The Building Earthquake Ground Motion level have earthquake location with a 10% probability of exceedance in 50 years (recurrence period of 475 years) movement level. Further, Local Soil Class C has very tight layers of sand, gravel, and hard clay or weathered, very cracked weak rocks. The following factors and coefficients have been applied to analyze the building behavior when subjected to earthquakes. The applied factors and coefficients according to TBEC-2018 [45] are given in Table 6.

Table 3. Frame section property definitions

Name	Mat.	Depth/Width (cm)	Bars	Design Type	Name	Mat.	Depth/Width (cm)	Bars	Design Type
BEAM 30X70	C16	70/30		Beam	S17-GRNDFL	C16	20/100	6ϕ16	Col.
BEAM20X60	C16	60/20		Beam	S1-BASEM.	C16	20/70	6ϕ16	Col.
S10-1	C16	20/60	6ϕ14	Col.	S1-GRNDFL	C16	20/60	6ϕ16	Col.
S10-2	C16	20/40	6ϕ14	Col.	S2-1	C16	20/80	6ϕ16	Col.
S10-BASEM.	C16	20/70	6ϕ16	Col.	S2-2	C16	20/70	6ϕ16	Col.
S10-GRNDFL	C16	20/60	6ϕ14	Col.	S2-BASEM.	C16	25/100	8ϕ16	Col.
S1-1	C16	20/50	6ϕ14	Col.	S2-GRNDFL	C16	20/100	6ϕ16	Col.
S11-1	C16	20/60	6ϕ14	Col.	S3-1	C16	20/80	6ϕ16	Col.
S11-2	C16	20/50	6ϕ14	Col.	S3-2	C16	20/60	6ϕ14	Col.
S11-BASEM.	C16	20/80	6ϕ16	Col.	S3-BASEM.	C16	25/100	8ϕ16	Col.
S11-GRNDFL	C16	20/70	6ϕ16	Col.	S3-GRNDFL	C16	20/90	6ϕ16	Col.
S1-2	C16	20/40	4ϕ14	Col.	S4-1	C16	60/20	6ϕ14	Col.
S12-1	C16	90/20	6ϕ16	Col.	S4-2	C16	50/20	6ϕ14	Col.
S12-2	C16	40/20	6ϕ16	Col.	S4-BASEM.	C16	80/20	6ϕ16	Col.
S12-BASEM.	C16	100/30	8ϕ16	Col.	S4-GRNDFL	C16	70/20	6ϕ16	Col.
S12-GRNDFL	C16	100/20	6ϕ16	Col.	S5-1	C16	20/60	6ϕ14	Col.
S13-1	C16	60/20	6ϕ14	Col.	S5-2	C16	20/50	6ϕ14	Col.
S13-2	C16	40/20	6ϕ14	Col.	S5-BASEM.	C16	20/80	6ϕ16	Col.
S13-BASEM.	C16	70/20	6ϕ16	Col.	S5-GRNDFL	C16	20/70	6ϕ16	Col.
S13-GRNDFL	C16	60/20	6ϕ14	Col.	S6-1	C16	80/20	6ϕ16	Col.
S14-1	C16	20/60	6ϕ14	Col.	S6-2	C16	70/20	6ϕ16	Col.
S14-2	C16	20/40	6ϕ14	Col.	S6-BASEM.	C16	100/25	6ϕ14	Col.
S14-BASEM.	C16	20/70	6ϕ16	Col.	S6-GRNDFL	C16	100/20	6ϕ16	Col.
S14-GRDFL	C16	20/60	6ϕ14	Col.	S7-1	C16	50/20	4ϕ14	Col.
S15-1	C16	20/60	6ϕ14	Col.	S7-2	C16	40/20	4ϕ14	Col.
S15-2	C16	20/40	6ϕ14	Col.	S7-BASEM.	C16	70/20	6ϕ16	Col.
S15-BASEM.	C16	20/70	6ϕ16	Col.	S7-GRNDFL	C16	50/20	6ϕ14	Col.
S15-GRNDFL	C16	20/60	6ϕ14	Col.	S8-1	C16	60/20	6ϕ14	Col.
S16-1	C16	20/90	6ϕ14	Col.	S8-2	C16	50/20	6ϕ14	Col.
S16-2	C16	20/70	6ϕ16	Col.	S8-BASEM.	C16	80/20	6ϕ16	Col.
S16-BASEM.	C16	30/100	6ϕ16	Col.	S8-GRNDFL	C16	70/20	6ϕ16	Col.
S16-GRNDFL	C16	25/100	6ϕ14	Col.	S9-1	C16	20/80	6ϕ16	Col.
S17-1	C16	20/80	6ϕ16	Col.	S9-2	C16	20/70	6ϕ16	Col.
S17-2	C16	20/70	6ϕ16	Col.	S9-BASEM.	C16	25/100	6ϕ16	Col.
S17-BASEM.	C16	25/100	8ϕ16	Col.	S9-GRNDFL	C16	20/100	6ϕ16	Col.

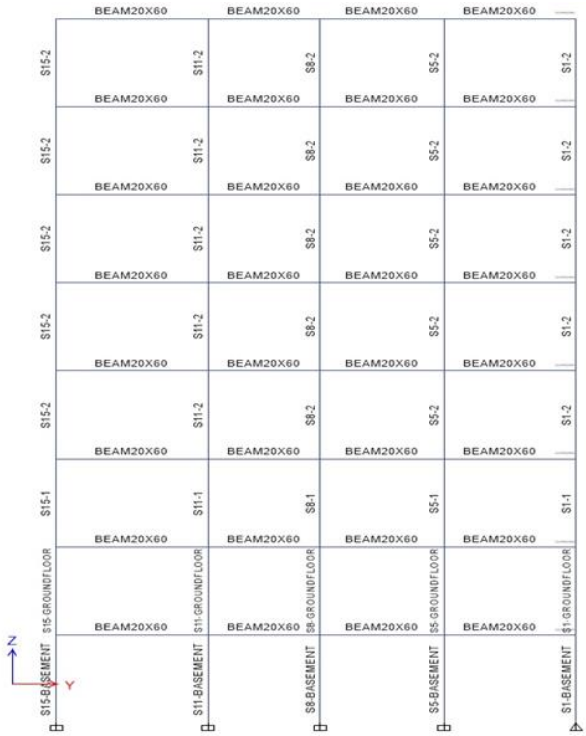

Fig. 9 Frame sections on the Y-Z plane

Table 4. Vibration periods and frequencies

Mode	Period (sec)	Frequency (cyc/sec)
1	1.232	0.812
2	1.058	0.945
3	1.011	0.99
4	0.41	2.44
5	0.355	2.819
6	0.336	2.981
7	0.243	4.111
8	0.21	4.752
9	0.195	5.127
10	0.17	5.884
11	0.146	6.854
12	0.133	7.537

Table 5. Joint properties of load-bearing elements on the 4th floor of the building

	A-B	B-IO (minimum)	IO-LS (pronounced)	LS-CP (advanced)	Total
Beam	0	79	0	0	79
Column	0	0	0	32	32

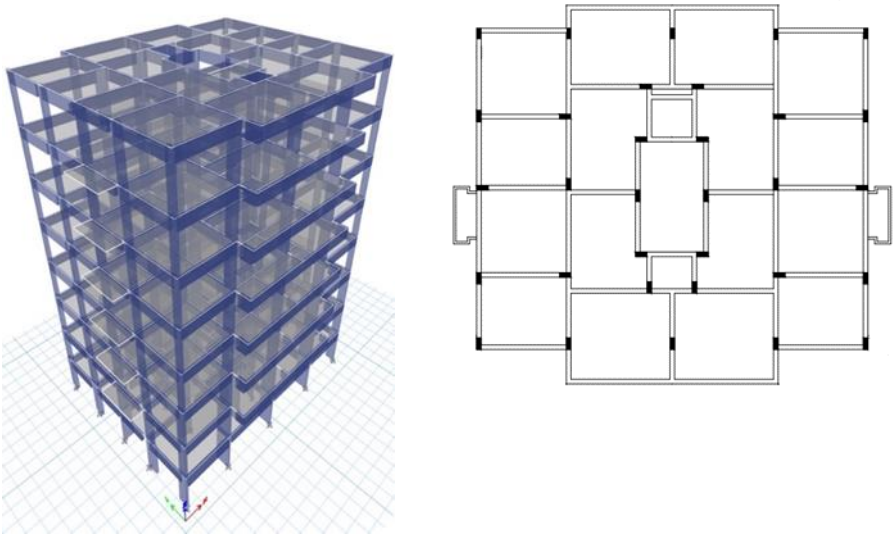

(a) (b)

Fig. 10 8-Story building (a) Model layout in ETABS, (b) Plan Layout

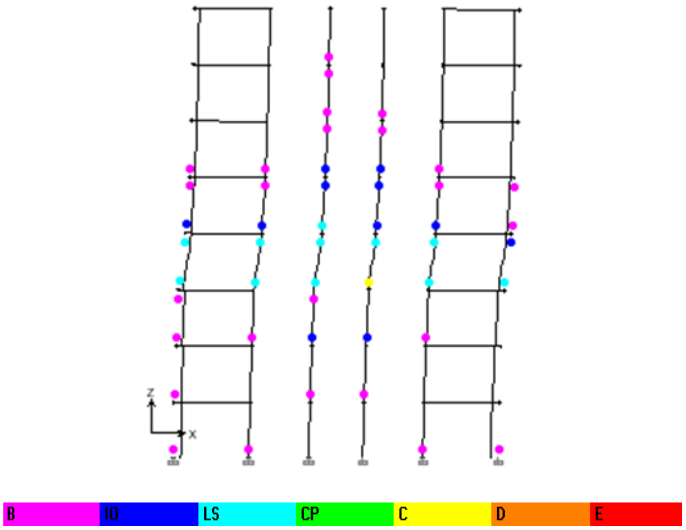

Fig. 11 Plastic hinges of the building - side view subjected to an earthquake event

Design spectral acceleration coefficients can be calculated by the following equations.

$$S_{DS} = S_S F_S \quad (1)$$

$$S_{D1} = S_1 F_1 \quad (2)$$

where, S_{DS} = Short period design spectral acceleration coefficient, S_{D1} = Design spectral acceleration coefficient for a period of 1.0 second, F_S = 1.2 (Site Coefficient (TBEC-2018 [45]: Table 2.1)), F_1 = 1.5 (Site Coefficient (TBEC-2018 [45]: Table 2.2))

Table 6. Applied Factor and coefficients according to TBEC-2018 [45].

Response Modification Factor (R)	4
System Overstrength Factor (Ω_0) 3	3
Importance Factor (I)	1
Short-period map spectral acceleration coefficient (S_S)	1.048
Map spectral acceleration coefficient for a 1.0 second period (S_1)	0.273
Maximum ground acceleration [g] (PGA)	0.445
Maximum ground speed [cm/sec] (PGV)	27.550

For this research, 11 pairs of ground motions shown in Table 7 were obtained from the PEER database [47] and the analyses were conducted by utilizing these motions. An earthquake-resistant structure's seismic design depends largely on the seismic response spectrum obtained from an earthquake-hazard analysis. Furthermore, an algorithm for generating realistic design acceleration time series is based on spectral matching in the time domain. For this study, the spectral matching method is applied with 5% damping by using SeismoMatch and ETABS programs to match the earthquake records to the target response band, the match is done according to the time domain and based on the [48].

Table 7. Selected earthquake records

No.	Earthquake	Year	Magnitude	Rjb (km)	Rrup (km)	Peer No.
1	"Duzce_Türkiye"	1999	7.14	12.02	12.04	1602
2	"Friuli_ Italy-01"	1976	6.5	33.32	33.4	122
3	"Imperial Valley-06"	1979	6.53	15.19	15.19	164
4	"Kern County"	1952	7.36	38.42	38.89	15
5	"Kobe_Japan"	1995	6.9	24.85	24.85	1100
6	"Kocaeli_Türkiye"	1999	7.51	10.56	13.49	1148
7	"Landers"	1992	7.28	34.86	34.86	838
8	"Loma Prieta"	1989	6.93	39.32	39.51	762
9	"Manjil_Iran"	1990	7.37	12.55	12.55	1633
10	"Morgan Hill"	1984	6.19	23.23	23.24	450
11	"Northridge-01"	1994	6.69	35.66	36.77	942

Nonlinear time-history analyses were performed to estimate and evaluate the performance of the strengthened structure in compliance with TBEC-2018 [45] code specifications. The obtained results are used to determine whether the strengthened structure will survive and sustain earthquakes more than the normal structure.

3. Analysis Results and Discussion

A variety of results of NLTHA have been carried out considering a set of 11 accelerograms matching on both original and strengthened buildings, which are discussed, and compared to demonstrate the effectiveness of employing the proposed SHARK energy absorber in seismic strengthening.

The seismic responses, considered for investigation and comparison, includes story displacement, drift, and acceleration as well as input energy to the building. All the selected earthquake records have been subjected to the buildings as X-X Y-Y which is the X-Direction of the building and X-direction of the earthquake and Y-direction of the building and Y-direction of the earthquake. Furthermore, X-Y Y-X is the X-Direction of the building and Y-direction of the earthquake and Y-direction of the building and X-direction of the

earthquake. As stated by TBEC-2018 [45] which indicate that at least eleven earthquake ground motion sets are used in nonlinear calculations to be made in the time history.

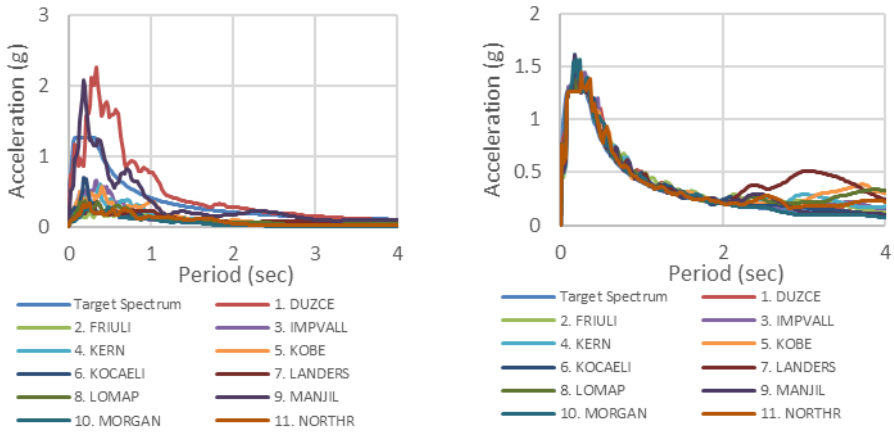

Fig. 12 The unscaled and scaled response spectrum of all earthquakes (x-direction)

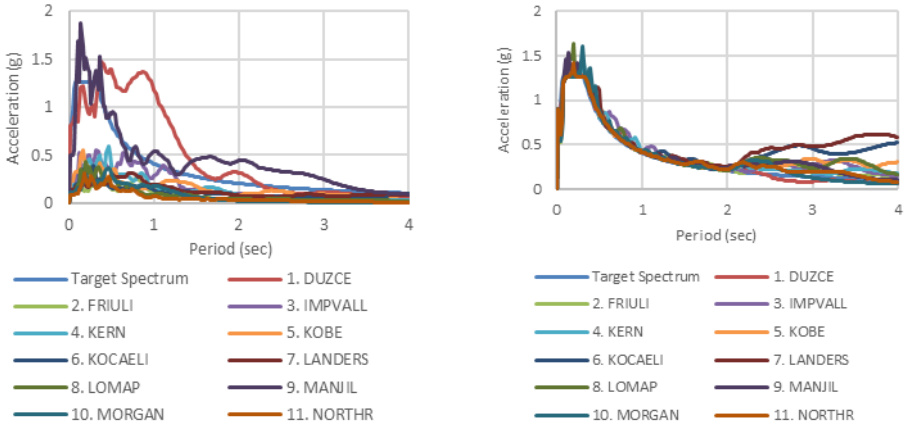

Figure 13. The unscaled and scaled response spectrum of all earthquakes (y-direction)

Acceleration records in two perpendicular horizontal directions are applied simultaneously in the direction of the (X) and (Y) principal axes of the system. Then, the axes of the acceleration records are rotated 90° and the calculations are repeated.

Figure 14 demonstrates the applied energy absorber configurations (CONF1, CONF2) which are used in the strengthening of the building. The connection of the SHARK device is applied to the beams and the bottom ends of the columns. As a representative of the numerical results of NLTHA, the time histories and responses of the buildings subjected to the DUZCE X-X Y-Y earthquake are presented in Figures 15-19.

For economical design, parameters of the smallest size of the energy absorber of SHARK (see Table 2) are used in the modelling of both configurations.

Figures 15 to 19 demonstrated that the implementation of SHARK in the building resulted in a considerable response. As can be seen in Figures 15a and 15b the time history response has resulted in a significant reduction of the Top Story Displacement for DUZCE X-X Y-Y in the X and Y directions of the building, respectively.

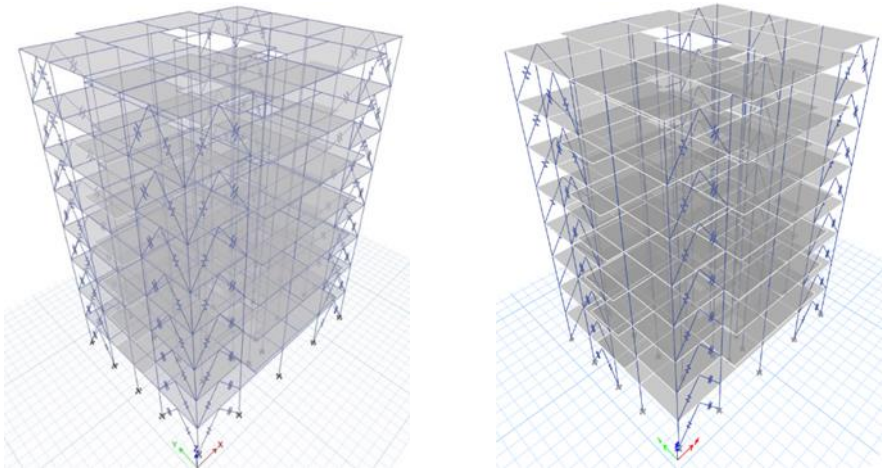

Fig. 14 8-Story building with two SHARK configurations a) CONF1, b) CONF2

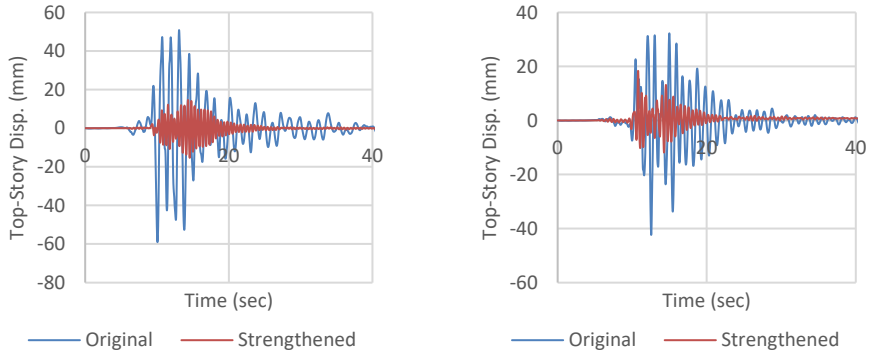

Fig. 15 Top-story displacement (DUZCE X-X Y-Y, CONF1) a) in the X-dir., b) in the Y-dir.

Further, Figures 16a and 16b showed a minimal reduction of the Top Story Acceleration for DUZCE X-X Y-Y in the X and Y directions of the building, respectively. However, in some cases during minor *Serviceability Limit State* (SLS) events, the SHARK generally operates within its elastic range and behaves like a stiff restrainer without much reduction of the earthquake input. This performance characteristic can lead to an increment of the peak story acceleration, which can be prejudicial to the non-structural components and technological contents for buildings such as hospitals, fire stations, police stations, data centers, emergency centers, or substantial commercial structures. To address this issue, the SHARK-Adaptive configuration can be utilized at a higher cost when compared to SHARK [32].

Moreover, Figures 17 and 18 demonstrate all stories' responses to displacement and drift. Figures 17 and 18 showed that there was significant displacement and drift reductions of all stories in both the X- and Y- direction of the building, respectively. Lastly, Figure 19 demonstrated the considerable input energy reduction of the strengthened building when compared to the original building.

In the interest of succinctness, this paper does not present graphical results for all the considered earthquakes that were applied. Instead, the maximum responses of the stories

under the applied scaled earthquakes are presented in Table 8 in X- and Y-directions of the building.

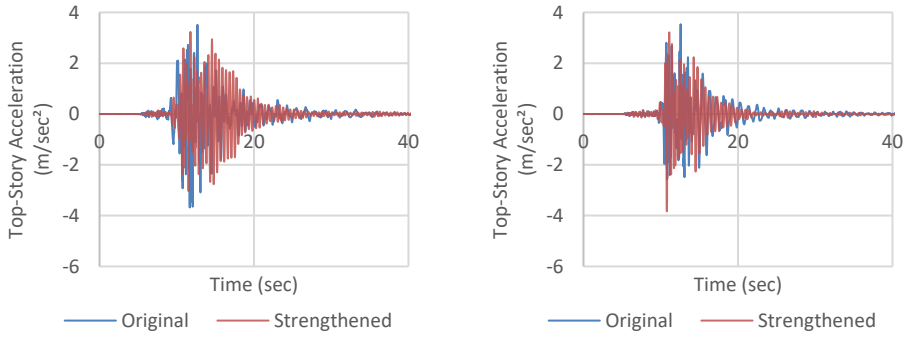

Fig. 16 Top-story acceleration (DUZCE X-X Y-Y, CONF1) a) in the X-dir., b) in the Y-dir.

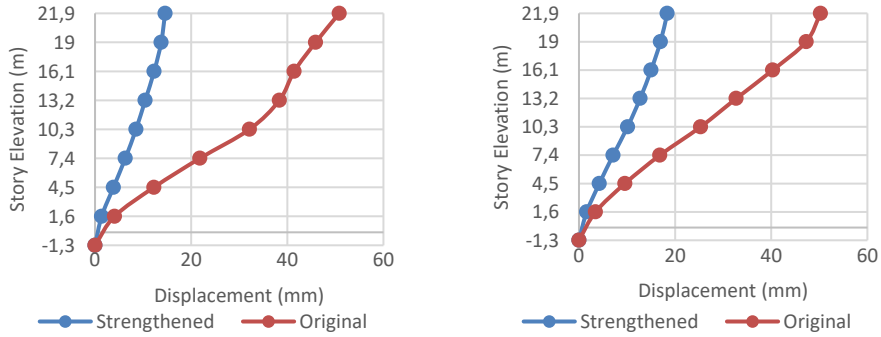

Fig. 17 Stories displacement (DUZCE X-X Y-Y, CONF1) a) in the X-dir., b) in the Y-dir.

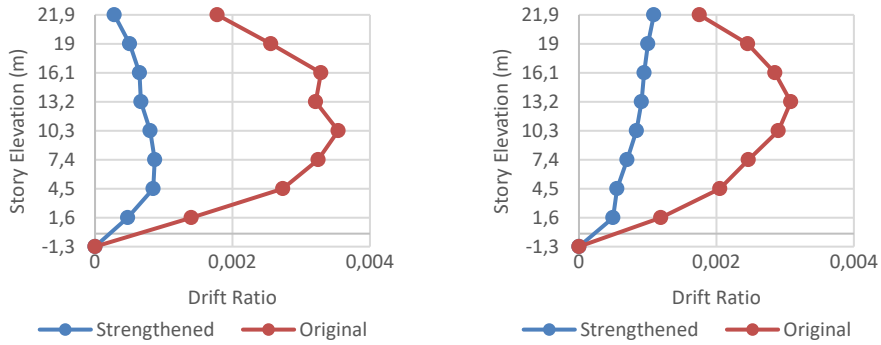

Fig. 18 Stories drift (DUZCE X-X Y-Y, CONF1) a) in the X-dir., b) in the Y-dir.

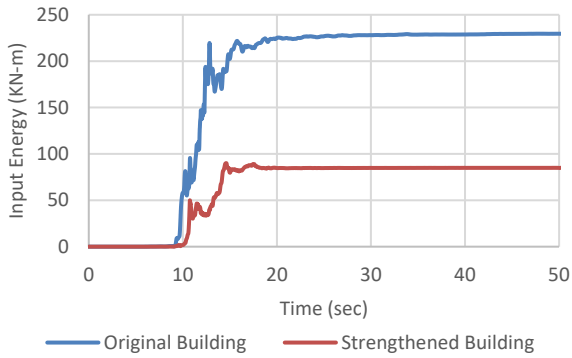

Fig. 19 Input energy to the building in the original and strengthened model with CONF1 (DUZCE X-X Y-Y)

Table 8 demonstrated the maximum responses of the 8-Story original and strengthened with configuration 1 buildings for story displacement, story drift, and story acceleration, all of which are significantly decreased compared to the original building. The reduction of the displacement in most of the cases is over 70% for the X-direction, while, in the Y-direction most of the cases are over 60%. The reduction of the drift in most of the cases is over 80% for the X-direction, while, in the Y-direction most of the cases are over 70%. Furthermore, the reduction of the acceleration in the X-direction varied between 8% to 44%, but in some cases showed below 1% reduction, while in the Y-direction varying between 4% to 28%. Further, 3 of the cases in the X-direction resulted in acceleration increments varying between 7% to 22%. While in the Y-direction 9 of the cases resulted in acceleration increments of 0.3% and 27%. The acceleration increment can be due to the fact the SHARK performance characteristic may behave like a stiff restrainer in some earthquake events which led to an increment of the story acceleration, or it can be due to long-period earthquakes, because of the close correlation between the period of the strengthened building and some of the selected earthquakes. Nevertheless, most of the strengthened building results have shown significantly better seismic performance than the original building results, which approve of the effectiveness of SHARK as an energy dissipation device.

The input energy caused by earthquakes subjected to original and strengthened buildings is shown in Table 9. According to the results, the strengthened building showed a significant decrease in the input energy as compared to the original building.

Table 8. Max story response in X- and Y-direction of the building with CONF1

Output Case		X-Direction			Y-Direction		
		Story Disp. (mm)	Story Drift (Ratio)	Story Acc. (m/sec^2)	Story Disp. (mm)	Story Drift (Ratio)	Story Acc. (m/sec^2)
1. DUZCE X-X Y-Y	Original	50.81	0.001778	3.27	50.26	0.001752	3.56
	Strength.	14.58	0.000281	2.9	18.37	0.000495	2.73
Reduction %		71	84	11	63	72	23
1. DUZCE X-Y Y-X	Original	73.24	0.002688	4.38	46.97	0.001374	4.08
	Strength.	12.545	0.000243	2.64	17.89	0.000488	2.93
Reduction %		83	91	40	62	64	28
2. FRIULI X-X Y-Y	Original	60.32	0.002108	2.88	49.9	0.001746	3.82
	Strength.	16.08	0.000347	3.51	18.27	0.000501	3.32
Reduction %		73	83	-22	63	71	13
2. FRIULI X-Y Y-X	Original	67.65	0.002437	3.55	42.23	0.001539	2.84
	Strength.	15.46	0.000316	3.16	18.25	0.000473	3.9
Reduction %		77	87	11	57	69	-37
3. IMPVAL X-X Y-Y	Original	65.87	0.002333	3.52	49.87	0.001598	2.83
	Strength.	13.68	0.000293	2.62	16.94	0.000456	2.5
Reduction %		79	87	26	66	71	12
3. IMPVAL X-Y Y-X	Original	64.1	0.002025	3.64	46.63	0.001381	2.83
	Strength.	14.51	0.000282	2.82	16.39	0.000467	2.98
Reduction %		77	86	22	65	66	-5
4. KERN X-X Y-Y	Original Strengthened	72.1	0.002195	4.8	44.21	0.001355	2.62
		15.98	0.000322	3.46	17.33	0.000483	3.32
Reduction %		78	85	28	61	64	-27
4.KERN X-Y Y-X	Original	56.05	0.001999	2.82	52.11	0.001464	3.55
	Strength.	13.67	0.000307	2.81	15.98	0.000463	2.74
Reduction %		76	85	0.35	69	68	23
5.KOBE X-X Y-Y	Original	68.45	0.002648	4.7	48.96	0.001451	3.12
	Strength.	16.13	0.000349	3.6	14.77	0.000418	2.88
Reduction %		76	87	23	70	71	8
5. KOBE X-Y Y-X	Original	63.7	0.002387	3.12	41.94	0.001392	3.48
	Strength.	12.4	0.00028	2.88	16.02	0.00041	3.17
Reduction %		81	88	8	62	70	9
6. KOCAELI X-X Y-Y	Original	61.79	0.001786	4.35	41.23	0.001505	3.02
	Strength.	14.82	0.000303	3.02	12.06	0.000405	2.73
Reduction %		76	83	31	71	73	10
6. KOCAELI X-Y Y-X	Original	50.077	0.002164	3.11	42.35	0.001306	3.36
	Strength.	11.91	0.000238	2.6	16.08	0.000424	2.45
Reduction %		76	89	16	62	68	27
7. LANDERS X-X Y-Y	Original	63.73	0.002365	3.35	64.29	0.002458	3.66
	Strength.	15.54	0.000298	2.88	15.83	0.000441	2.96
Reduction %		76	87	14	75	82	19
7. LANDERS X-Y Y-X	Original	52.25	0.001851	3.19	45.73	0.001413	3.23
	Strength.	14.94	0.000339	3.41	16.31	0.000509	3.52
Reduction %		71	82	-7	64	64	-9
8.LOMA X-X Y-Y	Original	75.64	0.002401	4.06	41.38	0.001696	3.28
	Strength.	13.77	0.000292	3.04	17.71	0.000547	3.29
Reduction %		82	88	25	57	68	-0.3
8. LOMA X-Y Y-X	Original	73.8	0.00278	4.13	52.09	0.001554	3.5
	Strength.	13.52	0.000315	2.71	17.83	0.000525	3.37
Reduction %		82	87	34	66	66	4
9. MANJIL X-X Y-Y	Original	83.23	0.002287	3.73	53.33	0.001725	2.65
	Strength.	11.9	0.000266	2.5	19.16	0.000577	3.22
Reduction %		86	88	33	64	67	-22
9. MANJIL X-Y Y-X	Original	58.23	0.002207	3.25	51.4	0.001416	2.86
	Strength.	13.77	0.000301	2.8	16.81	0.000453	2.88
Reduction %		76	86	14	67	68	-0.7

10. MORGAN X-X Y-Y	Original	61.35	0.002433	4.11	31.72	0.001296	2.92
	Strength.	14.72	0.000281	2.48	17.47	0.000586	3.37
Reduction %		76	88	40	45	55	-15
10. MORGAN X-Y Y-X	Original	73.23	0.002769	2.41	54.83	0.001884	3.54
	Strength.	12.86	0.000256	2.77	18.07	0.000484	2.56
Reduction %		82	91	-15	67	74	28
11. NORTHR X-X Y-Y	Original	66.27	0.00286	3.6	49.65	0.001879	3.13
	Strength.	12.18	0.000285	2.97	14.39	0.000493	3.42
Reduction %		82	90	18	71	74	-9
11. NORTHR X-Y Y-X	Original	60.63	0.001949	3.8	41.66	0.001832	3.75
	Strength.	13.37	0.0003	2.95	17.92	0.000476	3.49
Reduction %		78	85	22	57	74	6

Table 9. Input energy to the building with the original model and CONF1

Output Case	Original kN-m	Strengthened kN-m	Reduction %
1. DUZCE X-X Y-Y	229.5858	90.0942	61
1. DUZCE X-Y Y-X	252.9478	113.9889	55
2. FRIULI X-X Y-Y	510.8472	153.1915	70
2. FRIULI X-Y Y-X	511.5960	208.5827	59
3. IMPVAL X-X Y-Y	1034.5741	257.7190	75
3. IMPVAL X-Y Y-X	829.4655	271.2382	67
4. KERN X-X Y-Y	483.8709	212.1759	56
4. KERN X-Y Y-X	555.8534	153.9982	72
5. KOBE X-X Y-Y	432.5402	109.6562	75
5. KOBE X-Y Y-X	469.9797	79.3143	83
6. KOCAELI X-X Y-Y	304.4265	86.4378	72
6. KOCAELI X-Y Y-X	221.4493	65.4920	70
7. LANDERS X-X Y-Y	324.9492	104.8087	68
7. LANDERS X-Y Y-X	336.4976	117.8001	65
8. LOMA X-X Y-Y	592.2024	191.5439	68
8. LOMA X-Y Y-X	589.2366	163.445	72
9. MANJIL X-X Y-Y	343.3354	100.8728	71
9. MANJIL X-Y Y-X	357.7581	119.9789	66
10 MORGAN X-X Y-Y	271.8399	99.4532	63
10 MORGAN X-Y Y-X	273.9571	104.7164	62
11. NORTHR X-X Y-Y	340.3192	115.6935	66
11. NORTHR X-Y Y-X	415.5953	138.7465	67

The variance of Inter Story Drift Ratio (ISDR) requirements along stories height of the strengthened building is shown in Table 10.

$$\Delta_i = u_i - u_{i-1} \tag{3}$$

$$\delta_i = \frac{R}{I}\Delta_i \tag{4}$$

$$\text{Max ISDR}\left(\frac{\delta_i}{h_i}\right) \leq \frac{0.008\,k}{\lambda} \tag{5}$$

A building's drift demand is calculated by subtracting the consecutive story displacements, resulting from the analysis of the building under earthquake effects as specified by Eq. (3). By using Eq. (4), the effective story drift can be determined. The maximum ratio of story drift to story height is calculated as specified in Eq. (5) to determine the maximum ISDR of the building. The ISDR limit resulted to be 2.6%.

According to the results, the ISDR in the X-direction of the original building showed that stories 3 and 4 have more than the ISDR limit. However, the strengthened building reduced the ISDR and performed within the limit. Furthermore, the ISDR for the strengthened building showed much less when compared to the original building. The strengthening of the building is also accomplished by the implementation of the most economical size of SHARK in Configuration 2 (CONF2) (see Figure 14b).

Table 10. ISDR in X- and Y- directions of the building with CONF1

	X-Direction				Y-Direction			
Story No.	Original ISDR	Limit Check	Strengthened	Limit Check	Original ISDR	Limit Check	Strengthened	Limit Check
8	0.013546	WL	0.001120	WL	0.008215	WL	0.001951	WL
7	0.012327	WL	0.002016	WL	0.019213	WL	0.002699	WL
6	0.008473	WL	0.002571	WL	0.020939	WL	0.003130	WL
5	0.017146	WL	0.002639	WL	0.020470	WL	0.003600	WL
4	0.028507	ML	0.003069	WL	0.023357	WL	0.004154	WL
3	0.026357	ML	0.003398	WL	0.020065	WL	0.003966	WL
2	0.022601	WL	0.003390	WL	0.016867	WL	0.003628	WL
1	0.011206	WL	0.001909	WL	0.009525	WL	0.002216	WL

WL: Within Limit, ML: More than Limit

Figures from 20 to 24 demonstrated the implementation of SHARK to the building in configuration 2 (CONF2). As it can be seen in figures 20a and 20b, the time history response has resulted in a significant reduction of the Top-Story Displacement for DUZCE X-X Y-Y in the X- and Y-directions of the building, respectively.

Further, Figures 21a and 21b showed a minimal reduction of the Top-Story Acceleration for DUZCE X-X Y-Y in the X- and Y-directions of the building, respectively. Moreover, figures 22 and 23 demonstrate all stories' responses to displacement and drift. These figures showed that there was a significant displacement and drift reduction of all stories in both the X- and Y-directions of the building. Lastly, figure 24 demonstrated the considerable input energy reduction of the strengthened building when compared to the original building. This paper does not present graphical results for all the considered earthquakes that were applied. Instead, the maximum responses of the stories are presented in Table 12 in the X- and Y-directions.

Table 12 demonstrated the maximum responses of the original and strengthened building with configuration 2. Story displacement, story drift, and story acceleration are significantly decreased compared to the original building. The reduction of the displacement in most of the cases is over 65% for the X-direction, while in the Y-direction, most of the cases are over 55%. The reduction of the drift in most of the cases is over 80% for the X-direction, while in the Y-direction, most of the cases are over 70%, which is the same as for configuration 1. Furthermore, the reduction of the acceleration in the X-direction in most of the cases varies between 3% to 42% while in the Y-direction, in most of the cases vary between 2% to 39%. Further, 4 of the cases in the X-direction resulted in an acceleration increment varying between 11% to 45%. 5 of the cases in the Y-direction resulted in an acceleration increment varying between 1% to 12%.

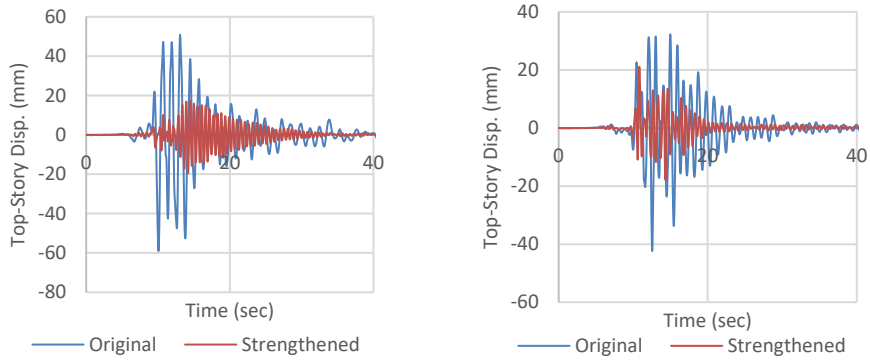

Fig. 20 Top-story displacement (DUZCE X-X Y-Y, CONF2) a) in the X-dir., b) in the Y-dir.

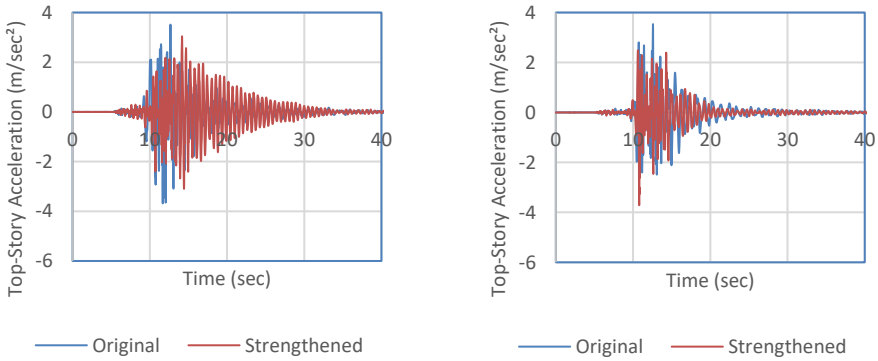

Fig. 21 Top-story acceleration (DUZCE X-X Y-Y, CONF2) a) in the X-dir., b) in the Y-dir.

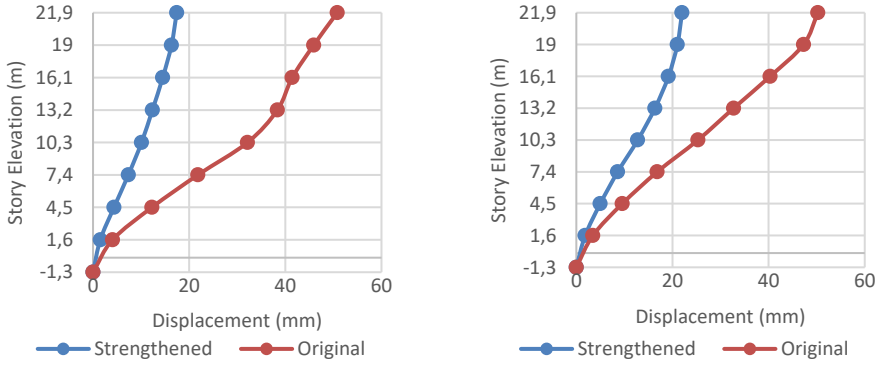

Fig. 22 Stories displacement (DUZCE X-X Y-Y, CONF2) a) in the X-dir., b) in the Y-dir.

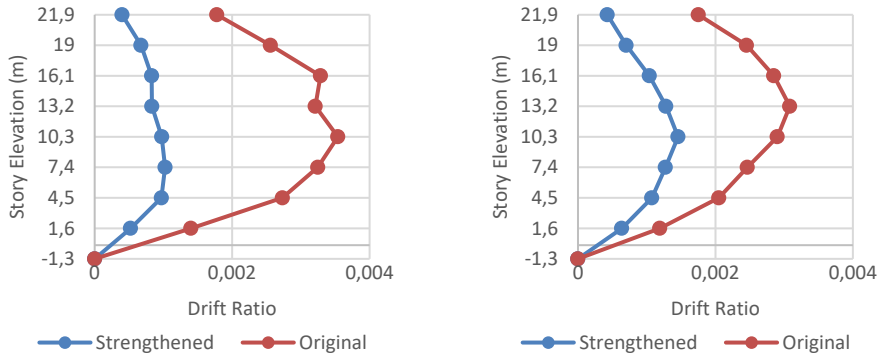

Fig. 23 Stories drift (DUZCE X-X Y-Y, CONF2) a) in the X-dir., b) in the Y-dir.

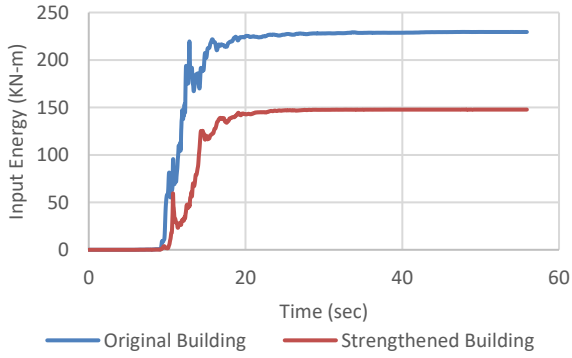

Fig. 24 Input energy to the building in the original and strengthened model with CONF2 (DUZCE X-X Y-Y)

By comparing the results of configuration 1 and configuration 2, it can be seen that displacement and drift results are very close. However, the acceleration results in the X-direction showed that there is a slight difference with the acceleration reduction percentage, but there is more acceleration increment percentage for configuration 2. While the Y-direction showed that configuration 1 has better performance in the acceleration reduction when compared to configuration 2. As mentioned earlier, the slight difference in the acceleration reduction can be due to SHARK performance may behave like a stiff restrainer in some earthquake events, in which this issue can be addressed by the usage adaptive shark which can provide effective protection of non-structural components and technological content of the building because of the flexible damper response (minimization of peak floor accelerations) under weak but frequent Serviceability Limit State (SLS) earthquakes. In addition, the acceleration increment percentage could be due to long-period earthquakes because of the close correlation between the period of the strengthened building and some of the selected earthquakes. Nevertheless, both configurations have shown significantly better seismic performance than the original ones, which approves the effectiveness of SHARK as an energy dissipation device in both configurations.

Table 12. Max story response in X- and Y-direction of the building with CONF2

Output Case		X-Direction			Y-Direction		
		Story Disp. (mm)	Story Drift (Ratio)	Story Acc. (m/sec^2)	Story Disp. (mm)	Story Drift (Ratio)	Story Acc. (m/sec^2)
1. DUZCE X-X Y-Y	Original	50.81	0.001778	3.27	50.26	0.001752	3.56
	Strengthened	17.41	0.000398	2.9	21.08	0.000428	2.61
Reduction %		66	78	11	58	76	27
1. DUZCE X-Y Y-X	Original	73.24	0.002688	4.38	46.97	0.001374	4.08
	Strengthened	19.21	0.000403	3.03	15.22	0.000336	2.49
Reduction %		74	85	31	68	75	39
2. FRIULI X-X Y-Y	Original	60.32	0.002108	2.88	49.9	0.001746	3.82
	Strengthened	17.89	0.000349	3.21	15.74	0.00034	2.37
Reduction %		70	83	-11	68	80	38
2. FRIULI X-Y Y-X	Original	67.65	0.002437	3.55	42.23	0.001539	2.84
	Strengthened	19.67	0.000453	3.21	17.4	0.000367	2.66
Reduction %		71	81	10	59	76	6
3. IMPVAL X-X Y-Y	Original	65.87	0.002333	3.52	49.87	0.001598	2.83
	Strengthened	18.39	0.000437	2.99	18.44	0.000431	2.93
Reduction %		72	81	15	63	73	-3
3. IMPVAL X-Y Y-X	Original	64.1	0.002025	3.64	46.63	0.001381	2.83
	Strengthened	17.4	0.000367	2.92	15.59	0.000339	2.5
Reduction %		73	82	20	67	75	12
4. KERN X-X Y-Y	Original	72.1	0.002195	4.8	44.21	0.001355	2.62
	Strengthened	16.53	0.000353	3.27	20.1	0.000435	2.93
Reduction %		77	84	32	55	68	-12
4.KERN X-Y Y-X	Original	56.05	0.001999	2.82	52.11	0.001464	3.55
	Strengthened	19.65	0.00042	3.67	19.52	0.000366	2.91
Reduction %		65	79	-30	62	75	18
5.KOBE X-X Y-Y	Original	68.45	0.002648	4.7	48.96	0.001451	3.12
	Strengthened	17.5	0.000369	3.17	17.2	0.000291	2.38
Reduction %		74	86	32	65	80	24
5. KOBE X-Y Y-X	Original	63.7	0.002387	3.12	41.94	0.001392	3.48
	Strengthened	14.96	0.000358	2.49	19.6	0.00041	2.85
Reduction %		76	85	20	53	71	18
6.KOCAELI X-X Y-Y	Original	61.79	0.001786	4.35	41.23	0.001505	3.02
	Strengthened	18.36	0.000361	2.53	15.39	0.000357	3.06
Reduction %		70	80	42	63	76	-1.3
6. KOCAELI X-Y Y-X	Original	50.077	0.002164	3.11	42.35	0.001306	3.36
	Strengthened	12.59	0.000262	2.79	19.77	0.000369	2.97
Reduction %		75	88	10	53	72	12
7. LANDERS X-X Y-Y	Original	63.73	0.002365	3.35	64.29	0.002458	3.66
	Strengthened	18.29	0.000482	4.44	17.22	0.000318	2.24
Reduction %		71	80	-32	73	87	39
7. LANDERS X-Y Y-X	Original	52.25	0.001851	3.19	45.73	0.001413	3.23
	Strengthened	17.04	0.000327	2.52	16.76	0.000341	2.36
Reduction %		67	82	21	63	76	27
8.LOMA X-X Y-Y	Original	75.64	0.002401	4.06	41.38	0.001696	3.28
	Strengthened	18.82	0.000424	2.96	17.32	0.000427	2.79
Reduction %		75	82	27	58	75	15
8. LOMA X-Y Y-X	Original	73.8	0.00278	4.13	52.09	0.001554	3.5
	Strengthened	19.01	0.000447	3.28	15.94	0.000402	2.32
Reduction %		74	84	21	69	74	34
9. MANJIL X-X Y-Y	Original	83.23	0.002287	3.73	53.33	0.001725	2.65
	Strengthened	18.65	0.000383	3.22	18.38	0.000413	2.74
Reduction %		78	83	14	65	76	-3.4

9. MANJIL X-Y Y-X	Original	58.23	0.002207	3.25	51.4	0.001416	2.86
	Strengthened	19.34	0.000524	3.07	16.24	0.000419	2.79
Reduction %		67	76	6	68	70	2
10. MORGAN X-X Y-Y	Original	61.35	0.002433	4.11	31.72	0.001296	2.92
	Strengthened	19.43	0.000429	3.08	18.95	0.000353	2.87
Reduction %		68	82	25	40	73	2
10. MORGAN X-Y Y-X	Original	73.23	0.002769	2.41	54.83	0.001884	3.54
	Strengthened	21.03	0.000488	3.5	15.27	0.000325	2.44
Reduction %		71	82	-45	72	83	31
11. NORTHR X-X Y-Y	Original	66.27	0.00286	3.6	49.65	0.001879	3.13
	Strengthened	16.94	0.000473	3.5	17.05	0.00031	2.89
Reduction %		74	83	3	66	83	8
11. NORTHR X-Y Y-X	Original	60.63	0.001949	3.8	41.66	0.001832	3.75
	Strengthened	18.78	0.000464	3.53	18.25	0.000343	3.79
Reduction %		69	76	7	56	81	-1

Table 13. Input energy to the building with the original model and CONF2

Output Case	Original kN-m	Strengthened kN-m	Reduction %
1. DUZCE X-X Y-Y	229.5858	147.7328	36
1. DUZCE X-Y Y-X	252.9478	96.6466	62
2. FRIULI X-X Y-Y	510.8472	183.0025	64
2. FRIULI X-Y Y-X	511.596	200.9595	61
3. IMPVAL X-X Y-Y	1034.5741	531.0618	49
3. IMPVAL X-Y Y-X	829.4655	378.2784	54
4. KERN X-X Y-Y	483.8709	293.0583	39
4. KERN X-Y Y-X	555.8534	305.6324	45
5. KOBE X-X Y-Y	432.5402	128.5034	70
5. KOBE X-Y Y-X	469.9797	145.0765	69
6. KOCAELI X-X Y-Y	304.4265	106.6303	65
6. KOCAELI X-Y Y-X	221.4493	108.9572	51
7. LANDERS X-X Y-Y	324.9492	111.8569	66
7. LANDERS X-Y Y-X	336.4976	101.8414	70
8. LOMA X-X Y-Y	592.2024	257.867	56
8. LOMA X-Y Y-X	589.2366	204.2867	65
9. MANJIL X-X Y-Y	343.3354	178.379	48
9. MANJIL X-Y Y-X	357.7581	170.0593	52
10 MORGAN X-X Y-Y	271.8399	151.0671	44
10 MORGAN X-Y Y-X	273.9571	123.1499	55
11. NORTHR X-X Y-Y	340.3192	199.1478	41
11. NORTHR X-Y Y-X	415.5953	215.1773	48

The input energy caused by earthquakes subjected to the original and strengthened buildings as in Configuration 2 is shown in Table 13. According to the results, the strengthened building showed a significant decrease in the input energy as compared to the original building.

The variance of ISDR requirements along stories height of the 8-Story strengthened building is shown in Table 14. The building's drift demand is calculated by subtracting the

consecutive story displacements, resulting from the analysis of the building under earthquake effects. According to the results, the ISDR requirements should be less than 2.6%, which is a limit according to TBEC-2018 [45].

Table 14. ISDR in X- and Y-directions of the building with CONF2

	X-Direction				Y-Direction			
Story No.	Original ISDR	Limit Check	Strengthened	Limit Check	Original ISDR	Limit Check	Strengthened	Limit Check
8	0.013546	WL	0.001506	WL	0.008215	WL	0.001346	WL
7	0.012327	WL	0.002509	WL	0.019213	WL	0.002556	WL
6	0.008473	WL	0.002965	WL	0.020939	WL	0.003874	WL
5	0.017146	WL	0.003104	WL	0.02047	WL	0.004936	WL
4	0.028507	ML	0.003789	WL	0.023357	WL	0.005742	WL
3	0.026357	ML	0.004122	WL	0.020065	WL	0.005008	WL
2	0.022601	WL	0.003928	WL	0.016867	WL	0.004327	WL
1	0.011206	WL	0.00209	WL	0.009525	WL	0.002551	WL

WL: Within Limit, ML: More than Limit

According to the results, the ISDR in the X-direction of the original building showed that stories 3 and 4 have more than the ISDR limit. However, the strengthened building reduced the ISDR and performed within the limit. Furthermore, the ISDR for the strengthened building showed much less when compared to the original building.

4. Conclusions

This study carried out a procedure that includes model calibration parameters obtained from the analysis of ambient vibration records for seismic strengthening of multi-story existing RC buildings. This was done through the implementation of the SHARK Hysteretic Energy Dissipation Device. The proposed procedure for design and configurations has been evaluated through NLTHA by applying a pair of 11 selected earthquake records on an 8-Story RC building without and with SHARK. The implementation of the SHARK has been carried out in two configurations by the usage of the specified sizes and values that are provided by MAURER [41] and applied in the ETABS program to achieve the proper behavior of the energy dissipation system against earthquakes. First, the X- and Y-components of the earthquakes were applied to the X- and Y-directions of the building, and then the components of the earthquakes are rotated 90° and reapplied to the X- and Y-directions of the building. It was observed that the seismic responses of the strengthened structure were significantly higher than the original structure. The levels of input energy decreased considerably, and the structure was able to resist various earthquake events with less displacement, drift ratio, and acceleration. The following conclusions can be derived from the results of the conducted NLTHA:

- The maximum displacement reduction values of the strengthened building are between 70% and 80% in comparison to the original building. The reduction is on average about 78% and 72% for the x-direction. However, the y-direction resulted in a 64% and 62% reduction for CONF1 and CONF2, respectively.
- The maximum drift reduction values of the strengthened building are between 70% and 80% in comparison to the original building. The reduction is on average about 87% and 82% for the x-direction. However, the y-direction resulted in a 69% and 76% reduction for CONF1 and CONF2, respectively.
- The maximum acceleration reduction values of the strengthened building are between 4% and 20% compared to the original building. The reduction is on average about 17% and 10% for the x-direction of the building with CONF1 and CONF2, respectively. Furthermore, there were some cases with acceleration increment which can be due to the fact that the SHARK performance characteristic may behave like a stiff restrainer in some earthquake events which led to an

increment of the story acceleration. This issue can be addressed by the usage of adaptive-shark which can provide effective protection of non-structural components and technological content of the building because of the flexible damper response (minimization of peak floor accelerations) under weak but frequent Serviceability Limit States earthquakes. This beneficial performance is essential for very important buildings (e.g., hospitals, police stations, fire stations, data centers, important commercial structures, or emergency management centers) that are required to remain fully operational in the emergency response after an earthquake. In addition, the increase in acceleration in some cases can be due to long-period earthquakes, because of the close correlation between the period of the strengthened building and some of the selected earthquakes. Nevertheless, most of the strengthened building cases have shown significantly better seismic performance than the original one, which approves the effectiveness of SHARK as an energy dissipation device.

- The input energy of the strengthened building showed a significant decrease as compared to the original building. The reduction is on average about 64% and 70% for the 8-Story building with CONF1 and CONF2, respectively.
- All the results of the Inter Story Drift Ratio ISDR of the strengthened building are obtained less than the estimated limit according to TBEC-2018.

Based on the above conclusions, the use of the proposed MAURER SHARK-which provides high protection of the structure during severe Ultimate Limit State earthquakes, long-term reliability against wear and fatigue problems, high redundant safety level, easy visual inspection, and easy-to-replace at low cost- is highly recommended, either for seismic strengthening of the existing buildings or newly designed ones. Finally, it should be emphasized that this study was limited to a few multi-story RC buildings. For more encompassing conclusions, this study should be expanded to encompass several buildings.

The comprehensive analytical work conducted in this research has improved the understanding of earthquake effects on buildings, building behavior, seismic strengthening, and hysteretic energy absorbers. However, some investigation needs to be addressed. Further research studies in this area are recommended as follows:

- In this research, Non-Linear Time History Analysis is performed on a three-dimensional system model and then the building is strengthened. But the building model was a simplified model of a real building with basic structural framing which didn't include various elements such as walls, elevators, stairs, etc. A better realistic model can be used to get accurate results and perform safer strengthening.
- When the SHARK experiences minor serviceability limit states (SLS), like other conventional bilinear dampers, the damper primarily operates in its elastic range, acting as a stiff restraint without reducing the input of the earthquake. Therefore, it's recommended to use the SHARK-Adaptive configuration to address this issue effectively.
- Applying different installation configurations than the studied ones can give acceptable results with fewer Energy Dampers for more economical strengthening of old or designing new buildings.

It's recommended to make a study on the cost evaluation of applying the MAURER devices to the new and old buildings.

References

[1] El-Betar SA. Seismic vulnerability evaluation of existing RC buildings. HBRC Journal, 2018; 14(2), 189-197. https://doi.org/10.1016/j.hbrcj.2016.09.002

[2] Gökkaya K. Geographic analysis of earthquake damage in Turkey between 1900 and 2012. Geomatics, Natural Hazards and Risk, 2016; 7(6), 1948-1961. https://doi.org/10.1080/19475705.2016.1171259
[3] Isik V, Uysal IT, Caglayan A, Seyitoglu G. The evolution of intraplate fault systems in central Turkey: Structural evidence and Ar-Ar and Rb-Sr age constraints for the Savcili Fault Zone. Tectonics, 2014; 33(10), 1875-1899. https://doi.org/10.1002/2014TC003565
[4] Atmaca B, Demir S, Gunaydin M, Altunisik AC, Husem M, Ates S. Angin Z. Lessons learned from the past earthquakes on building performance in Turkey, Journal of Structural Engineering & Applied Mechanics, 2020; 3(2), 61-84. https://doi.org/10.31462/jseam.2020.02061084
[5] Bulut F, Aktuğ B, Yaltırak C, Doğru A, Özener H. Magnitudes of future large earthquakes near Istanbul quantified from 1500 years of historical earthquakes, present-day microseismicity and GPS slip rates. Tectonophysics, 2019; 764, 77-87. https://doi.org/10.1016/j.tecto.2019.05.005
[6] Mojarab M, Memarian H, Zare M. Performance evaluation of the M8 algorithm to predict M7+ earthquakes in Turkey. Arabian Journal of Geosciences, 2015; 8(8), 5921-5934. https://doi.org/10.1007/s12517-014-1624-3
[7] Cagatay IH. Experimental evaluation of buildings damaged in recent earthquakes in Turkey. Engineering Failure Analysis, 2005; 12(3), 440-452. https://doi.org/10.1016/j.engfailanal.2004.02.007
[8] Pinho R. Selective retrofitting of RC structures in seismic areas, Ph.D. Thesis, Faculty of Engineering, University of London, 2000, London.
[9] Tsionis G, Apostolska R, Tauver F. Seismic strengthening of RC buildings, Publications Office of European Union, 2014, Luxembourg.
[10] Benjamin JR, Cornell CA. Probability, statistics, and decisions for civil engineers. Dover Publications, 2014.
[11] Veletsos A, Newmark NM. Effect of inelastic behavior on the response of simple systems to earthquake motions. Second World Conference on Earthquake Engineering, 1960; 2: 895-912 Tokyo, Japan.
[12] Castaldo P. Integrated seismic design of structure and control systems. Springer, 2014. https://doi.org/10.1007/978-3-319-02615-2
[13] Constantinou MC, Soong TT, Dargush GF. Passive energy dissipation systems for structural design and retrofit, University of Buffalo, USA, 1998.
[14] Gkournelos P, Triantafillou T, Bournas D. Seismic upgrading of existing reinforced concrete buildings: A state-of-the-art review. Engineering Structures, 2021; 240, 112273. https://doi.org/10.1016/j.engstruct.2021.112273
[15] Franco J, Cahís X, Gracia L, López F. Experimental testing of a new anti-seismic dissipator energy device based on the plasticity of metals. Engineering structures, 2010; 32(9), 2672-2682. https://doi.org/10.1016/j.engstruct.2010.04.037
[16] Dolce M, Cardone D, Ponzo FC, Valente C. Shaking table tests on reinforced concrete frames without and with passive control systems. Earthquake Engineering and Structural Dynamics, 2005; 34(14), 1687-1717. https://doi.org/10.1002/eqe.501
[17] Reinhorn AM, Li C, Constantinou M. Experimental and analytical investigation of seismic retrofit of structures with supplemental damping: Part. 1-fluid viscous damping devices. Thecnical Report NCEER-95-0001, University of Buffalo, USA, 1995.
[18] Aiken ID, Nims DK, Whittaker AS, Kelly JM. Testing of passive energy dissipation systems. Earthquake Spectra, 1993; 9(3), 335-370. https://doi.org/10.1193/1.1585720
[19] Khampanit A, Leelataviwat S, Kochanin J, Warnitchai P. Energy-based seismic strengthening design of non-ductile reinforced concrete frames using buckling-restrained braces. Engineering Structures, 2014; 81(4), 110-122. https://doi.org/10.1016/j.engstruct.2014.09.033

[20] Sahoo DR, Rai DC. Seismic strengthening of non-ductile reinforced concrete frames using aluminum shear links as energy-dissipation devices. Engineering Structures, 2010; 32(11), 3548-3557. https://doi.org/10.1016/j.engstruct.2010.07.023
[21] Ghandil M, Riahi HT, Behnamfar F. Introduction of a new metallic-yielding pistonic damper for seismic control of structures. J. Constr. Steel Res. 2022; 194, 107299. https://doi.org/10.1016/j.jcsr.2022.107299
[22] Sabelli R, Mahin S, Chang C. Seismic demands on steel braced frame buildings with buckling-restrained braces. Engineering Structures, 2003; 25(5), 655-666. https://doi.org/10.1016/S0141-0296(02)00175-X
[23] Tsai KC, Chen HW, Hong CP, Su YF. Design of steel triangular plate energy absorbers for seismic-resistant construction. Earthquake spectra, 1993; 9(3), 505-528. https://doi.org/10.1193/1.1585727
[24] Titirla MD. Using Friction-Yielding Damper CAR1 to Seismic Retrofit a Two-Story RC Building: Numerical Application. Applied Sciences, 2023; 13(3), 1527. https://doi.org/10.3390/app13031527
[25] Di Cesare A, Ponzo FC, Nigro, D. Assessment of the performance of hysteretic energy dissipation bracing systems. Bulletin of Earthquake Engineering, 2014; 12(6), 2777-2796. https://doi.org/10.1007/s10518-014-9623-z
[26] Di Cesare A, Ponzo FC. Seismic retrofit of reinforced concrete frame buildings with hysteretic bracing systems: design procedure and behaviour factor. Shock and Vibration, 2017. https://doi.org/10.1155/2017/2639361
[27] Tena-Colunga A, Nangullasmú-Hernández H. Assessment of seismic design parameters of moment resisting RC braced frames with metallic fuses. Engineering Structures, 2015; 95, 138-153. https://doi.org/10.1016/j.engstruct.2015.03.062
[28] Thongchom C, Mirzai N, Chang B, Ghamari A. Improving the CBF brace's behavior using I-shaped dampers, numerical and experimental study. Journal of Constructional Steel Research, 2022; 197, 107482. https://doi.org/10.1016/j.jcsr.2022.107482
[29] Demir S, Husem M. Saw type seismic energy dissipaters: development and cyclic loading test. Journal of Constructional Steel Research, 2018; 150, 264-276. https://doi.org/10.1016/j.jcsr.2018.08.015
[30] Chen Y, Ye D, Zhang L. (2022). Analytical development and experimental investigation of the casting multi-plate damper (CMPD). Engineering Structures, 2022; 250, 113402. https://doi.org/10.1016/j.engstruct.2021.113402
[31] Zhang A, Ye Q. Design and testing of prefabricated steel frame with an innovative re-centering energy dissipative brace. Engineering Structures, 2019; 201, 109791. https://doi.org/10.1016/j.engstruct.2019.109791
[32] Gandelli E, Chernyshov S, Distl J, Dubini P, Weber F, Taras A. Novel adaptive hysteretic damper for enhanced seismic protection of braced buildings. Soil Dynamics and Earthquake Engineering, 2021; 141, 106522. https://doi.org/10.1016/j.soildyn.2020.106522
[33] Shih MH, Sung WP. Seismic Resistance and Parametric Study of Building under Control of Impulsive Semi-Active Mass Damper. Applied Sciences, 2021; 11(6), 2468. https://doi.org/10.3390/app11062468
[34] Bruschi E, Quaglini V, Zoccolini L. Seismic Upgrade of Steel Frame Buildings by Using Damped Braces. Applied Sciences, 2023; 13(4), 2063. https://doi.org/10.3390/app13042063
[35] Cao XY, Feng DC, Wu G, Wang Z. Experimental and theoretical investigations of the existing reinforced concrete frames retrofitted with the novel external SC-PBSPC BRBF sub-structures. Engineering Structures, 2022; 256, 113982. https://doi.org/10.1016/j.engstruct.2022.113982
[36] Cao XY, Feng DC, Wu G, Wang Z. Parametric investigation of the assembled bolt-connected buckling-restrained brace and performance evaluation of its application into

structural retrofit. Journal of Building Engineering, 2022; 48, 103988. https://doi.org/10.1016/j.jobe.2022.103988
[37] Nasab M, Guo YQ, Kim J. Seismic retrofit of a soft first-story building using viscoelastic dampers considering inherent uncertainties. Journal of Building Engineering, 2022; 47, 103866. https://doi.org/10.1016/j.jobe.2021.103866
[38] Thongchom C, Bahrami A, Ghamari A, Benjeddou O. Performance Improvement of Innovative Shear Damper Using Diagonal Stiffeners for Concentrically Braced Frame Systems. Buildings, 2022; 12(11), 1794. https://doi.org/10.3390/buildings12111794
[39] Zhu X, Wang W, Li W, Zhang Q, Du Y, Yin Y. Experimental and numerical study of X-type energy dissipation device under impact loads. Journal of Constructional Steel Research, 2023; 204, 107876. https://doi.org/10.1016/j.jcsr.2023.107876
[40] Zhang J, Fang C, Yam M, Lin C. Fe-Mn-Si alloy U-shaped dampers with extraordinary low-cycle fatigue resistance. Engineering Structures, 2022 264, 114475. https://doi.org/10.1016/j.engstruct.2022.114475
[41] MAURER SHARK® Short-Stroke Hysteretic Damper, 2020. Retrived from MAURER: https://www.maurer.eu/en/products/seismic-devices/dampers/index.html
[42] Genes MC, Gülkan PH, Bikçe M, Kaçın S. Combination of Instrumental and Numerical Data Based on the Mixed Approach of Reinforced Concrete Framed Structures Investigation of Damage and Seismic Characteristics, Tubitak (107M445)-IntenC Project final report, 2011.
[43] EN 15129 Anti-seismic devices, 2009.
[44] ACI 318-11 Building Code Requirements for Structural Concrete (ACI 318-11), An ACI Standard and Commentary. American Concrete Institute. Farmington Hills, USA, 2011.
[45] TBEC Türkiye Earthquake Code for Buildings. Disaster and emergency management presidency. Ministry of Interior, Ankara, Turkey, 2018.
[46] ASCE 41-17 Seismic evaluation and retrofit of existing buildings. American Society of Civil Engineers, USA, 2017.
[47] PEER Peer ground motion database. Pacific Earthquake Engineering Research Center. http://ngawest2.berkeley.edu. University of California, Berkeley, CA, USA, 2021.
[48] ASCE 7-16 Minimum Design Loads and Associated Criteria for Buildings and Other Structures, American Society of Civil Engineers, USA, 2017.